# Optical spectra and electronic structure of crystalline and glassy $Ge(S,Se)_2$

D. E. Aspnes, J. C. Phillips, and K. L. Tai
*Bell Laboratories, Murray Hill, New Jersey 07974*

P. M. Bridenbaugh
*Bell Laboratories, Holmdel, New Jersey 07733*
(Received 19 May 1980)

Dielectric-function spectra from 1.5 to 5.8 eV are reported for evaporated ($g$-)$GeSe_2$ films, ($c$-)$GeSe_2$ single crystals, and evaporated Ag-doped photoactivated $GeSe_2$ films. $c$-$GeSe_2$ is dichroic, yielding two spectra that we relate to the components of the dielectric tensor parallel and perpendicular to the $-GeSe-$ chains in this material. The dielectric function of $g$-$GeSe_2$ shows two broad peaks, which closely resemble the $c$-$GeSe_2$ spectra. Except for fine structure, the $g$-$GeSe_2$ spectrum can be synthesized from the $c$-$GeSe_2$ spectra in the effective-medium approximation. All structures are described by a simple model consisting of two narrow ($\sim 1$ eV) valence bands and a lower conduction band. Spectra for Ag-doped films have only a single broad peak in $\epsilon_2$. These results point to the existence of medium-range order in $g$-$GeSe_2$, in agreement with a recent theory which ascribes much greater order to the glass than is commonly expected on the basis of "random" network models.

## I. INTRODUCTION

Compounds and alloys of the chalcogenide elements S, Se, and Te form semiconductors over a wide range of compositions. The concentration of point defects in these materials (as determined, e.g., by paramagnetic resonance) can be very low, $\leq 10^{16}/cm^3$, even when they are prepared in an amorphous form. (For comparison, the concentration of similar defects in amorphous Si is typically $10^{19}/cm^3$.) It is likely that this low concentration of point defects is associated with the pronounced glass-forming tendency of the alloys, which is most marked[1] in the $As_x(S,Se)_{1-x}$ system at $x=0.4$ and in the $Ge_y(S,Se)_{1-y}$ system at $y=\frac{1}{6}$.

The aim of this paper is to investigate structural properties and chemical bonding in one member of this interesting family of materials. We have chosen $Ge(S,Se)_2$ because of several factors. (1) The dominant structural units in the crystals are corner-sharing tetrahedra, $Ge(Se_{1/2})_4$. Thus this material is similar in some respects to the canonical glass former, $SiO_2$, which also contains corner-sharing tetrahedra as its dominant structural unit. (2) The presence of tetrahedra simplifies the analysis of the local molecular structure. By contrast, in $a$-Se one finds both chains $Se_m$ of variable length and $Se_8$ rings.[2] In evaporated $a$-$As_2Se_3$ one learns from Raman and infrared spectroscopy that $As_4Se_4$ molecular units are present in substantial concentrations as a native molecular defect.[3] (3) Photoresists have been prepared[4,5] from $Ge_ySe_{1-y}$ alloys containing Ag. The resists prepared from these alloys appear to be much more sensitive than those prepared from $As_xSe_{1-x}$ alloys. This suggests some differences in these materials which we hope to elucidate.

The reflectance spectra of glassy $Ge_ySe_{1-y}$ alloys ($0\leq y\leq 0.33$) in the region $1.5\leq\hbar\omega\leq 5.5$ eV have been reported by Lannoo and Bensoussan (LB).[6] The reflectance spectrum of Se shows a plateau between 2.4 and 4.6 eV. With increasing amounts of Ge the low-energy corner of the plateau shifts upward to 2.7 eV at $y=0.33$, and the high-energy corner is replaced by increased reflectance (second absorption band) with a knee near 5 eV. No fine structure is evident in the glassy spectra, and no data are reported for the crystalline compound.

## II. EXPERIMENT

High-quality $GeSe_2$ single crystals were grown in the manner previously described by Bridenbaugh *et al.*[7] The as-grown crystals had natural cleavage faces that were flat, of high optical quality, and of the order of $5\times 10$ mm$^2$ in area. Because $c$-$GeSe_2$ is micaceous we assume that the natural cleavage face is in the layer plane.

$GeSe_2$ films were prepared by bulk evaporation from a baffled Ta boat in a background pressure not

 

exceeding $10^{-6}$ Torr. Typical deposition rates were 600 Å/min, and typical film thicknesses were 1–3 $\mu$m. The films were verified to be noncrystalline by electron beam and x-ray scattering measurements.

Optical data were taken using a rotating-analyzer ellipsometer described in detail elsewhere.[8] All measurements were performed on as-grown surfaces of evaporated films or on freshly cleaved surfaces of single-crystal samples. The samples were enclosed in a windowless cell containing a dry $N_2$ ambient to minimize possible surface-contamination effects. The stability and reproducibility of the spectra for any given sample showed these to be negligible. The accuracy of the data is determined almost entirely by sample variations such as microscopic inhomogeneities (voids) in evaporated samples and possible microscopic surface roughness in all samples. If sample-to-sample variations are a reliable guide, the results presented here should be accurate to within 5%.

## III. RESULTS AND DISCUSSION

### A. Complex dielectric function of $g$-$GeSe_2$

The real and imaginary parts of the complex dielectric function of $g$-$GeSe_2$ are shown in Fig. 1. The solid-line portions of these data were calculated directly from the ellipsometric data in the standard two-phase (ambient-isotropic substrate) model. The dashed-line parts lie in the region of transparency of the film and could not be obtained this way owing to multiple internal reflections. The dielectric-function spectra in this region were inferred from the amplitude and period of the interference oscillations. Also shown for comparison is the imaginary part of the dielectric function in the threshold region calculated from transmission measurements of a similar sample deposited on a fused-quartz substrate.

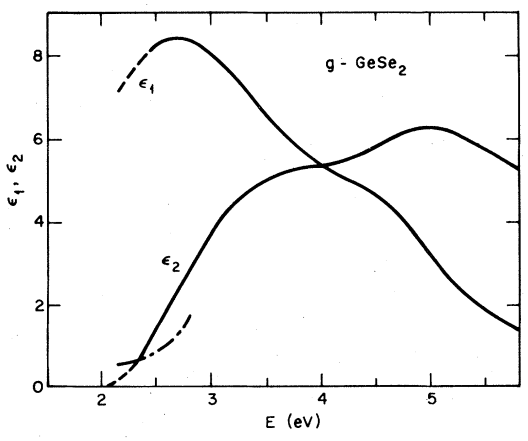


FIG. 1. Dielectric function for $g$-$GeSe_2$. Values of $\epsilon_2$ deduced from transmission measurements are shown from 2.1 to 2.7 eV.

The $\epsilon_2$ spectrum is characterized by a fairly abrupt threshold at about 2.2 eV, rising to a peak at 3.5 eV and followed by a second threshold and peak at about 4 and 5 eV, respectively. The double-peaked nature of the $\epsilon_2$ spectrum is in striking contrast to those of evaporated amorphous films of group IV and III–V semiconductors, which invariably show only a single broad peak.[9] It rather is reminiscent of those of amorphous films of the lone-pair materials Se and Te, which show two broad peaks separated by about 4 eV.[10] In the band-structure calculation of LM,[6] the first rise in the $g$-$GeSe_2$ spectrum would correspond to optical transitions between the $\tau$ (LM notation) lone-pair states of Se atoms to the $s$-like antibonding lower conduction band, and the second rise to transitions from the $p$-bonding valence to $s$-antibonding conduction band. The calculations also predict a possible structure midway between those observed due to $\tau$-antibonding $p$ transitions but this is not seen.

### B. Dielectric response of $c$-$GeSe_2$

Crystalline $GeSe_2$ is optically biaxial. Therefore, the principal components of the dielectric tensor cannot be measured individually by ellipsometry, because the complex reflection ratio is influenced by all three even if two of the principal axes lie in the plane of incidence. Although procedures have been developed[11] for computing these components from multiple ellipsometric measurements, these procedures require extremely accurate data obtained from undamaged, clean, and specular surfaces perpendicular to each of the three principal axes—a formidable challenge with a micaceous crystal. Our measurements, as noted above, were restricted to natural cleavage planes. This guarantees, however, that the plane of incidence always contains the principal axis normal to the surface, which we denote as the $b$ axis according to the usual convention.[12]

But under certain conditions, a rigorous analysis is not required. A pseudo-(apparent) dielectric-function spectrum, $\langle\epsilon(\omega)\rangle$, calculated in the two-phase model from data obtained with the plane of incidence containing in addition one of the two remaining principal axes in the plane of the surface, can provide an accurate estimate of the component of the dielectric tensor along the intersection between the surface and the plane of incidence.[13] Direct experimental evidence for such a separation of dielectric tensor components can be seen in Figs. 2 and 3. These figures show pseudodielectric-function spectra calculated from data taken with the plane of incidence parallel and perpendicular, respectively, to the –GeSe– chains

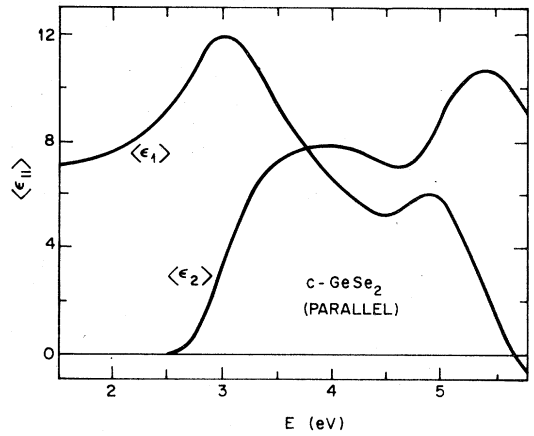


FIG. 2. Pseudodielectric function $\langle\epsilon\rangle_{\parallel}$ for $c$-$GeSe_2$. "Parallel" means that the plane of incidence is parallel to the –GeSe– chains of the crystal.

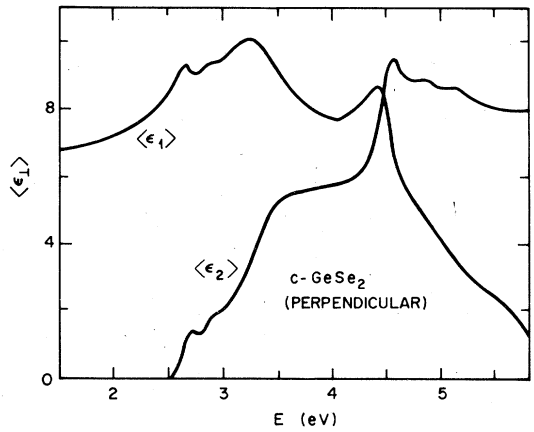


FIG. 3. Pseudodielectic function $\langle\epsilon\rangle_{\perp}$ for $c$-$GeSe_2$. "Perpendicular" means that the plane of incidence is perpendicular to the –GeSe– chains of the crystal.

in the material, as verified by x-ray orientation. In subsequent discussions we shall denote these as being the $\parallel$ and $\perp$ components, respectively. The complete lack of common structures in these spectra shows that they are essentially independent and are not linear combinations of more fundamental components. Specifically, the absorption edges occur at different energies and show fine structure in Fig. 3 but not in Fig. 2. Also, there is no evidence of structure at 4.4 eV in Fig. 2 corresponding to the relatively sharp threshold at this energy in Fig. 3.

The separation can be understood and the dominant dielectric tensor component identified by a straightforward calculation based on the theory of propagation of light in a biaxial medium. We suppose that the $xz$ plane is the plane of incidence, with the $z$ axis normal to the surface. This places the $s$-wave polarization field along $y$. Let the dielectric functions $\epsilon_i$ be given by $\epsilon+\Delta\epsilon_i$, $i=x$, $y$, or $z$, where $\epsilon$ is some mean or average value. Then the pseudodielectric function, $\langle\epsilon\rangle$, is given to first order in the corrections $\Delta\epsilon_i$ by[13]

$$\langle\epsilon\rangle=\epsilon+[(\epsilon-\sin^2\phi)\Delta\epsilon_x-(\epsilon\cos^2\phi-\sin^2\phi)\Delta\epsilon_y]/[\sin^2\phi(\epsilon-1)]-\Delta\epsilon_z/(\epsilon-1)\ , \tag{1}$$

where $\phi$ is the angle of incidence. Equation (1) shows that the correction to $\epsilon$ from the $z$ component is of order $|\epsilon|^{-1}$, that is, $\sim 0.1$ by Figs. 2 and 3. Therefore its contribution is minor, as is well known for uniaxial crystals.[14] But Eq. (1) shows further that the correction from the $y$ component is also small, because the two terms in the prefactor of $\Delta\epsilon_y$ virtually cancel for the values of $\langle\epsilon\rangle$ in Figs. 2 and 3 at the experimental angle of incidence $\phi=67.08°$.

We conclude that $\langle\epsilon\rangle\cong\epsilon+\Delta\epsilon_x=\epsilon_x$. Therefore, our pseudodielectric functions are indeed rather accurate measures of single components of the dielectric tensor, the components being those in plane of incidence and parallel to the surface for each of the two orientations used here. Thus the observed independence in Figs. 2 and 3 is understood and the proper tensor components are identified. We note that "parallel" and "perpendicular" now also refer to tensor components along and transverse to, respectively, the –GeSe– chains, as well as the orientation of the plane of incidence.

We now consider the dielectric response in more detail. Figures 2 and 3 show $c$-$GeSe_2$ to be dichroic, with two well defined, distinct absorption edges for electric fields lying in the cleavage plane and parallel and perpendicular to the –GeSe– chains. The lower-energy, perpendicular threshold in Fig. 3 shows distinct fine structure suggestive of a *triplet* of edges equally spaced $270\pm50$ meV apart and beginning at 2.54 eV. The higher-energy, parallel edge in Fig. 2 occurs at 2.70 eV (between the strong 2.54-eV and 2.81-eV thresholds) and shows *no* evidence of fine structure. The situation is effectively repeated at the higher-energy threshold, where the fine structure, or its absence, is again observed. The higher-lying thresholds are substantially more dichroic, being

separated by 0.4 eV. The broader structures of Fig. 2 also have about 60% more oscillator strength than the sharper structures of Fig. 3.

### C. Comparison of $g$-$GeSe_2$ and $c$-$GeSe_2$

The $c$-$GeSe_2$ dielectric-function spectra of Figs. 2 and 3 are compared to the $g$-$GeSe_2$ spectrum of Fig. 1 in Fig. 4. To simulate the latter, the $c$-$GeSe_2$ spectra have been combined in the Bruggeman effective-medium approximation,[15] using as free parameters the volume void fraction, $f_v$, and the relative fraction, $r$, of perpendicular (Fig. 3) to parallel (Fig. 2) dielectric responses. From linear regression analysis we find best-fit values of $f_v = 0.18 \pm 0.01$ and $r = 0.93 \pm 0.19$, where the uncertainties refer to 90% confidence levels in the parameters of the model. To obtain the fit as shown, the $c$-$GeSe_2$ spectra were also rigidly shifted 0.33 eV to lower energy.

The volume void fraction is significantly greater than the 10% density difference between glass and crystal.[16] However, this is entirely understandable because, by analogy to related layered materials,[17] the principal dielectric tensor component along $b$ is expected to be smaller than the other two. The larger apparent void fraction is simply an attempt by the model to reproduce the lower value of the $b$ component. It is reassuring that the relative proportions of the two components of the dielectric tensor that are available to us enter in nearly equal proportions ($r = 1$) to within the accuracy of determination of $r$. The shift to lower energy is suggestive of a general reduction in energy gaps due to the loss of long-range order

The overall agreement between data and calculation in Fig. 4 is remarkable. Not only are the two broad peaks reproduced, but also the relative proportions of parallel and perpendicular spectra are preserved and the value obtained for the apparent void fraction is consistent with expectations. Note also the similarities between spectra near and above 5 eV. In fact, the only features not preserved in the $g$-$GeSe_2$ spectrum are the fine structures that arise from the perpendicular spectrum of Fig. 3. A like situation is seen for $As_2Se_3$ where a close similarity in the dielectric functions of crystalline and glass phases has also been noted.[18] The evidence indicates the retention of a considerable fraction of order in the glass phase. We shall return to this point in Sec. III E.

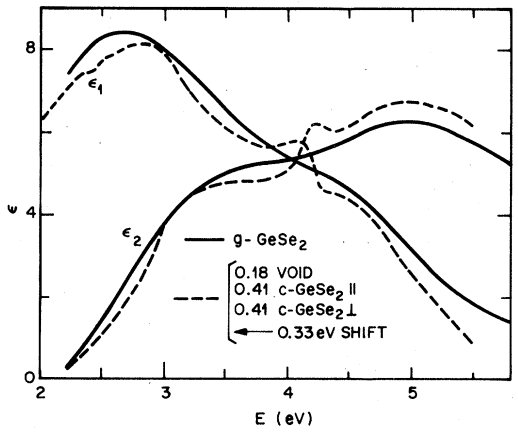


FIG. 4. Comparison of superposition of pseudodielectric functions $\langle\epsilon\rangle_{\parallel}$ and $\langle\epsilon\rangle_{\perp}$ of $c$-$GeSe_2$ with the dielectric function of $g$-$GeSe_2$ from Fig. 1, as described in the text.

### D. Theoretical models

The threshold structures in Fig. 3 are separated by an energy $\Delta_a = 270$ meV, which is similar to the $4p$ spin-orbit splittings[19] $\lambda$ of atomic Ge and Se and to the $p^{3/2}$-$p^{1/2} = \frac{3}{2}\lambda$ splitting[20] of 296 meV in $c$-Ge at the valence-band maximum. However, the lone-pair splitting of the $p_{\parallel}^2$ states is expected to give rise to a doublet of splitting $\lambda$. We suggest that the observed triplet may occur because there are[21] two structurally inequivalent Se atoms in $c$-$GeSe_2$, namely, Se($e$) which are members of 4-fold rings —Ge—Se—Ge—Se—, which occur in shared tetrahedral edges, and Se($c$) which are not contained in such rings and occur in shared tetrahedral corners. The Ge—Se($e$)—Ge bond angle[21] is only 80°, compared to 100° for Se($c$), which is close to the value for Se bond angles found[1] in elemental Se and in the dominant —AsSe— chains in $c$-$As_2Se_3$. Because Se($e$) is under strain we expect that lone-pair $4p$ valence-electron states localized on Se($e$) will have higher energy than those localized on Se($c$), while the final $s$-like conduction-band states (which are less sensitive to bond-angle distortions) will have similar energies. We therefore assign the $\alpha$ and $\beta$ absorption edges to spin-orbit split (and probably excitonic) states localized on Se($e$) atoms, while the $\gamma$ absorption edge is assigned to transitions originating on the Se($c$)atoms. We also note that each layer of $c$-$GeSe_2$ has a bilinear unit cell,[21] with the chains consisting of alternating Ge and Se($c$) atoms, while the Se($e$) atoms are isolated from the chains in cross-linking rings. If the lowest conduction-band states are localized more strongly on the chains, then the rapid linear rise in band-to-band absorption seen above the $\gamma$ edge can be easily understood.

To analyze the broad absorption bands at higher energies we focus our attention first on the parallel-polarized spectrum shown in Fig. 2. Although we do not have a direct measure of $\epsilon_2(\omega)$ above 5.8 eV, we can qualitatively estimate its behavior there from $\epsilon_1(\omega)$, which is determined in part through the Kramers-Kronig relations by values of $\epsilon_2(\omega)$ outside

the measurement range. By analogy to, e.g., amorphous Si,[22] the zero crossing of $\epsilon_1(\omega)$ at 5.7 eV provides good evidence that a substantial fraction of valence-conduction-band oscillator strength has been consumed by this energy, and that the pronounced rolloff of $\epsilon_2(\omega)$ beginning at 5.6 eV in Fig. 2 will continue to higher energies. We are therefore led to dissect the optical spectrum as shown in Fig. 5 into linear components arising from two valence bands ($A,B$) and one conduction band ($C$). Because the unit cell is so large we adopt the model relation

$$\epsilon_2(\omega) = \int [g_A N_A(\omega_1) + g_B N_B(\omega_1)] N_c(\omega_1+\omega) d\omega_1 , \tag{2}$$

which is analogous to the "nondirect-transition" model used previously to describe optical transitions in amorphous semiconductors.[9]

If the densities $N_A$, $N_B(N_c)$ have step-function behavior near their maxima (minima), as is reasonable for a layer structure, then the widths of $A$ and $B$ bands can be estimated from the widths of the linear threshold regions in $\epsilon_2^A$ and $\epsilon_2^B$, giving $W_A$ (upper valence band) $\approx 1$ eV and $W_B$ (second valence band) $\leq 1$ eV as well. From alloy data[6] it appears that the lower band involves partially Se (lone pair) $\rightarrow$ Se (antibonding) transitions, while the upper band probably involves second valence-band states which are partially centered on Ge atoms.

It is worth noting that the integrated oscillator strengths defined by

$$f_{A,B} = \frac{\pi}{2\omega_p^2} \int \omega [\epsilon_2(\omega)]_{A,B} d\omega , \tag{3}$$

where

$$[\epsilon_2(\omega)]_{A,B} = \int g_{A,B} N_{A,B}(\omega_1) N_c(\omega_1+\omega) d\omega_1 , \tag{4}$$

are approximately equal. Thus the lower band $A$ contains enough admixture of Ge $sp^3$ states into Se $p_\perp$ states to equal the spectral strength of the Se $p_\parallel^2$ states.

An interesting aspect of our spectral model for Fig. 2 is that it draws our attention to a feature of Fig. 3 which we might otherwise have overlooked, namely, in Fig. 3 $\epsilon_{2a}(\omega)$ is almost flat above 5 eV. This means that there is an additional absorption threshold in $\epsilon_{2a}(\omega)$ near 5.4 eV which is absent from $\epsilon_{2b}(\omega)$. We are tempted to ascribe this threshold to transitions from the upper valence band Se($e$) states to a high conduction $s$ band centered primarily on Se($e$), corresponding to the lower $s$ conduction band centered more heavily on Se($c$), as discussed above in connection with the $\alpha$, $\beta$, and $\gamma$ absorption edges. We note that this additional absorption band appears to be present in the glass spectrum shown in Fig. 1, which is consistent with the "outrigger-raft" model of the molecular structure of the glass recently proposed to explain Raman and diffraction data.[7] The much weaker fine structure ($\alpha, \beta, \gamma$) at the absorption edges in Fig. 3 is, however, absent in the glass because of inhomogeneous strains which deform the raft-structure energy levels on a scale of 0.05–0.1 eV.

### E. Dielectric response of Ag-doped photoactivated $g$-$GeSe_2$

Finally, we compare dielectric-function spectra of Ag-doped photoactivated $g$-$GeSe_2$ with that of the undoped material in Fig. 6. The two broad structures of $g$-$GeSe_2$ have now collapsed into the single broad peak characteristic of amorphous semiconductors having no lone-pair states. Yet except for the loss of broad structure and an increase in the magnitude of $\epsilon$, the dielectric responses of Ag-doped and undoped $g$-$GeSe_2$ are essentially the same.

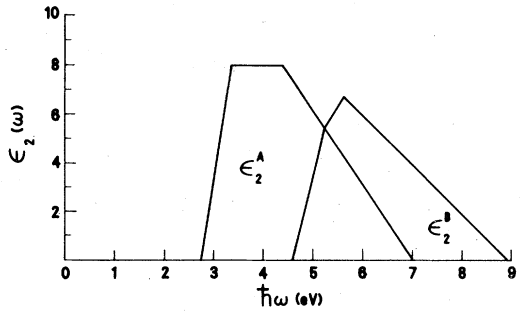


FIG. 5. Dissection of Fig. 3 into two components, the lower $\epsilon_2^A$ spectrum probably being derived from Se (lone pair) $\rightarrow$ Se (antibonding) transitions, the upper $\epsilon_2^B$ spectrum involving a mixture of Se and Ge initial valence states.

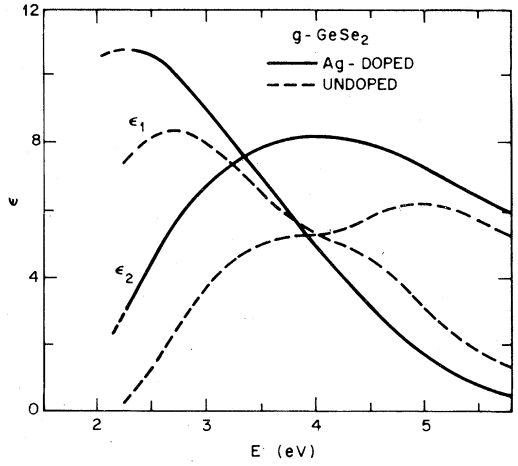


FIG. 6. Comparison of the dielectric-function spectrum of an Ag-photodoped $g$-$GeSe_2$ sample with that of undoped $g$-$GeSe_2$.

The general similarity of these spectra shows that the overall distribution of oscillator strength has not changed significantly by doping and photoactivation, indicating that the $Ge(Se_{1/2})_4$ tetrahedra are still the basic structural subunits. Recalling that the dielectric function is defined as polarization per unit volume, it is clear that the increase in magnitude of $\epsilon$ upon Ag doping results in either a more efficient packing (metallization) of these tetrahedra, or an increase in their polarizability at lower energies. Both effects are well documented for the polycrystalline-to-amorphous transition in Si,[23] where the loss of long-range order causes the two broad peaks in $\epsilon_2$ characteristic of the polycrystalline material to coalesce into a single, higher peak with a concomitant shift of the absorption edge to lower energy. The same behavior can be seen for $GeSe_2$ in Fig. 5. This, together with the fact that the $g$-$GeSe_2$ dielectric-function spectrum can be synthesized quite accurately from those of $c$-$GeSe_2$, indicates the existence of medium-range order in $g$-$GeSe_2$ which must be destroyed by photoactivation of the Ag dopant. Most probably, the Ag reduces the medium-range order by cutting the higher-energy bonds in the $-Ge-Se-Ge-Se-$ 4-fold rings of edge-sharing tetrahedra rather than breaking the corner-sharing links as the former are more highly strained.

In Se and Te, the bonding and lone-pair valence bands are separated by about 4 eV, as can be deduced from the energies of the respective peaks in the dielectric-function spectrum.[10] In $GeSe_2$, the separation is little more than 1.5 eV, as seen from Figs. 1–3. In $As_2Se_3$, the bonding and lone-pair bands are known to overlap and no (bonding)—(lone-pair) separation is seen in the optical spectra.[12,18] The effect of photoactivating Ag-doped $GeSe_2$ is to eliminate the separate peaks corresponding to bonding and lone-pair initial states, that is, to produce a material whose optical response is more nealy like that of $As_2Se_3$. If the conduction-band edge remains sharp to the scale of 1 eV for the photoactivated material, as seems likely, then the effect of the Ag and the photoactivation process is to blur the distinction between lone-pair and bonding orbitals. This argues further for a change in the local atomic structure, i.e., a loss of medium-range order that must have existed initially in the glass phase, and shows in addition that the Ag must be interacting primarily with Se. Thus a consistent picture is obtained.

## IV. CONCLUSIONS

While the optical spectra and electronic structure of chalcogenide compounds (such as $SnSe_2$) with the $CdI_2$-layered structure have received extensive attention,[24] because of the large number of atoms per unit cell there have been only a few studies of the electronic structure and optical spectra of $As_2Se_3$ (Refs. 12 and 18) and the single previous study[6] of the prototypical chalcogenide glass compound $GeSe_2$ succeeded only in separating Se transitions from those involving both Ge and Se. In the present work on $GeSe_2$ our ellipsometric data have presented for the first time both components of the complex dielectric function for the crystal and the average dielectric function of the glass. The polarization dependence in the layer plane of this bilinear material is sufficiently strong to have enabled us to identify specifically spectral features associated with edge-sharing tetrahedra as contrasted with corner-sharing tetrahedra, both at the direct absorption edge near 2.54 eV and in a strong absorption band near 5.5 eV.

Because the density of the glass is 10% less than that of the crystal[16] one might have expected the spectral features associated with edge-sharing tetrahedra to disappear in the glass. But we have discussed two results that provide rather persuasive evidence that medium-range order must be present in the glass. First, the dielectric-function spectrum of $g$-$GeSe_2$ can be synthesized rather accurately in the effective-medium approximation from those of $c$-$GeSe_2$, with reasonable values for the relative void and constituent polarization fractions. Second, the dielectric spectrum of Ag-doped $g$-$GeSe_2$ that has been photoactivated has only a single broad peak.

These observations are fully consistent with a recent model[7] of the molecular structure of $g$-$GeSe_2$ which ascribes much greater medium-range order to the glass than is commonly expected on the basis of "random" network models. While the present data are not sufficiently detailed to confirm or disprove the hypothesized partial breakdown[7] of chemical ordering[25] in $GeSe_2$ large molecular clusters, they do imply a much greater similarity of the structure of the dominant molecular clusters in the glass to the structure of the crystal than would be found from combinations of smaller molecular clusters, e.g., $Ge_2(Se_{1/2})_6$ units[26] or 12-atom alternating Ge-Se rings[27] which do not explain the companion Raman line.[7] In general our data support the view[7] that the structure of chalcogenide compound glasses [including $As_2Se_3$ (Ref. 28)] much more closely resembles the structure of the crystal than has been realized hitherto.

## ACKNOWLEDGMENT

We wish to thank S. H. Wemple for useful discussions on the dielectric properties of lone-pair materials, and for a critical reading of the manuscript.

[1]J. C. Phillips, J. Non-Cryst. Solids 34, 153 (1979).
[2]A. C. Wright and A. J. Leadbetter, Phys. Chem. Glasses 17, 122 (1976); M. F. Daniel, A. J. Leadbetter, A. C. Wright, and R. N. Sinclair, J. Non-Cryst. Solids 32, 271 (1979).
[3]A. J. Apling, A. J. Leadbetter, and A. C. Wright, J. Non-Cryst. Solids 23, 369 (1977).
[4]A. Yoshikawa, O. Ochi, H. Nagai, and Y. Mizushima, Appl. Phys. Lett. 31, 161 (1977).
[5]K. L. Tai, W. R. Sinclair, R. G. Vadimsky, J. M. Moran, and M. J. Rand, J. Vac. Sci. Technol. 16, 1977 (1979); K. L. Tai, R. G. Vadimsky, C. T. Kemmerer, J. S. Wagner, V. E. Lamberti, and A. G. Timko, *ibid.* 17, 1169 (1980).
[6]M. Lannoo and M. Bensoussan, Phys. Rev. B 16, 3546 (1977).
[7]P. M. Bridenbaugh, G. P. Espinosa, J. E. Griffiths, J. C. Phillips, and J. P. Remeika, Phys. Rev. B 20, 4140 (1979).
[8]D. E. Aspnes and A. A. Studna, Appl. Opt. 14, 220 (1975); SPIE J. 112, 62 (1978); Rev. Sci. Instrum. 49, 291 (1978); D. E. Aspnes, J. Opt. Soc. Am. 64, 812 (1974).
[9]M.-L. Theye, in *Optical Properties of Solids: New Developments,* edited by B. O. Seraphin (North-Holland, Amsterdam, 1976), p. 353.
[10]J. Stuke, J. Non-Cryst. Solids 4, 1 (1970).
[11]D. J. DeSmet, J. Opt. Soc. Am. 65, 542 (1975).
[12]H. L. Althaus, G. Weiser, and S. Nagel, Phys. Status Solidi B 87, 117 (1978).
[13]D. E. Aspnes, J. Opt. Soc. Am. 70, 1275 (1980).
[14]M. L. Jones, H. H. Soonpaa, and B. S. Rao, J. Opt. Soc. Am. 64, 1591 (1974).
[15]D. A. G. Bruggeman, Ann. Phys. (Leipzig) 24, 636 (1935).
[16]R. Azoulay, H. Thibierge, and A. Brenac, J. Non-Cryst. Solids 18, 33 (1975).
[17]GaSe: F. Meyer, E. E. de Kluizenaar, and D. den Engelsen, J. Opt. Soc. Am. 63, 529 (1973); graphite: E. A. Taft and H. R. Philipp, Phys. Rev. 138, A197 (1965).
[18]R. Zallen, R. E. Drews, R. L. Emerald, and M. L. Slade, Phys. Rev. Lett. 26, 1564 (1971).
[19]C. E. Moore, Nat. Bur. Stand. (U.S.), Circ. No. 467, Vol. II, pp. 135ff, 150ff (1952); G. G. Wepfer, T. C. Collins, and R. N. Euwema, Phys. Rev. B 4, 1296 (1971).
[20]D. E. Aspnes, Phys. Rev. B 12, 2297 (1975).
[21]G. Dittmar and H. Schafer, Acta Crystallogr. B 32, 2726 (1976).
[22]D. T. Pierce and W. E. Spicer, Phys. Rev. B 5, 3017 (1972).
[23]D. E. Aspnes, B. G. Bagley, A. C. Adams, and A. A. Studna, Bull. Am. Phys. Soc. 25, 12 (1980).
[24]R. H. Williams and A. W. Parke, J. Phys. C 11, 2549 (1978); I. C. H. Schluter and M. Schluter, Phys. Status Solidi B 57, 145 (1973).
[25]G. Lucovsky, R. J. Nemanich, and F. L. Galeener, in *Proceedings of the Seventh International Conference on Amorphous and Liquid Semiconductors, Edinburgh, 1977,* edited by W. E. Spear (University of Edinburgh, Edinburgh, 1977), p. 130.
[26]A. Feltz, B. Voigt, and E. Schlenzig, in *Proceedings of the Fifth International Conference on Amorphous and Liquid Semiconductors, West Germany, 1973,* edited by J. Stuke and W. Brenig (Taylor and Francis, London, 1974), p. 261.
[27]R. J. Nemanich, G. A. N. Connell, T. M. Hayes, and R. A. Street, Phys. Rev. B 18, 6900 (1978).
[28]J. C. Phillips, C. A. Beevers, and S. E. B. Gould, Phys. Rev. B 21, 5724 (1980).